GENERALIZED EQUIVALENT CIRCUIT MODEL FOR TRANSVERSE WAVEGUIDE SLOTS AND APPLICATIONS

I A. Eshrah, A. A. Kishk, A. B. Yakovlev, and A. W. Glisson

Department of Electrical Engineering
University of Mississippi
Anderson Hall 302, University, MS 38677, USA

Abstract—A generalized equivalent circuit model for waveguide transverse slots is proposed for the efficient analysis of waveguide transitions and waveguide slot antennas and slot-excited antennas. The transverse slots on the broad and end waveguide walls analyzed in this paper are decomposed into three structures: two apertures and an auxiliary waveguide section. The slot aperture in the host waveguide is modeled as an inductance-capacitance-transformer (LCT) combination, for which the equivalent inductance and capacitance are determined by first considering the case of zero-thickness slot, then the transformer turns ratio is calculated for the slot on a finite thickness wall. The effect of the wall thickness is accounted for by a waveguide section having cross-sectional dimensions equal to those of the slot, and length equal to the wall thickness. The loaded slot aperture is modeled along with the external load as a lumped load impedance. Expressions for the inductance, capacitance and transformer turns ratio are obtained in terms of the slot length and width. The obtained expressions facilitate the design of a variety of structures, including waveguide couplers, feeding networks and radiators. The equivalent circuit model proved to be accurate compared to the method of moments solution over a wide frequency band. Comparison of the scattering parameters obtained from the circuit analysis, the method of moments, and the finite-difference time-domain solutions exhibit very good agreement.

1. INTRODUCTION

Efficient and accurate analysis of finite arrays using equivalent circuit methods requires accurate modeling of the individual array elements. The availability of powerful circuit simulators, such as Agilent Advanced Design System (ADS) [1], motivates the development of equivalent circuit models for the array elements in order to take full advantage of the features provided by such simulators, not only to facilitate the design procedure, but also to gain more insight in the impact of the various design parameters on the system response. As array elements, waveguide slots were extensively studied [2–5], and various algorithms were proposed to design small or large slot arrays [6–8]. Recently, waveguide slots were used as an excitation mechanism, coupling the microwave power supported by the waveguide to an external radiator, such as a dielectric resonator antenna [9]. For such problems, an equivalent circuit model for the feeding structure, viz. the waveguide and the slot, can make the design process easier and more feasible, and facilitates the transition from the element analysis to the array analysis [10].

In previous work [11], the authors have proposed a simple LC equivalent circuit model for a waveguide slot coupler, where the circuit parameters were found to be constant over the whole frequency band of interest. Although the equivalent circuit of [11] produced results that are in excellent agreement with the full-wave analysis results, the model has a number of shortcomings: (a) the inductance and capacitance are functions of the slot thickness (the thickness of the wall where the slot exists) and the constitutive parameters characterizing the slot filling material, (b) the circuit parameters are functions of the dimensions and material parameters of *both* coupled waveguides, and (c) the model was only applied to coupling problems of two *identical* waveguides. The latter point is a major shortcoming in that model, as the main motivation behind the development of such model is alleviating the difficulties in the analysis of waveguide slot antenna arrays and waveguide slot-excited arrays of other radiators, such as dielectric resonator antennas [9]. The dependence of the equivalent circuit on the external load does not allow separate analysis of the feeding network and the array, which tremendously increases the difficulty of accurate design of such arrays.

In this work, a generalized equivalent circuit model for waveguide slots is presented, where the slot is viewed as three separate structures, namely, an aperture in the host waveguide, a waveguide section (the wall thickness), and an aperture loaded by some external load as shown in Fig. 1. The aperture in the host waveguide is modeled as an LC
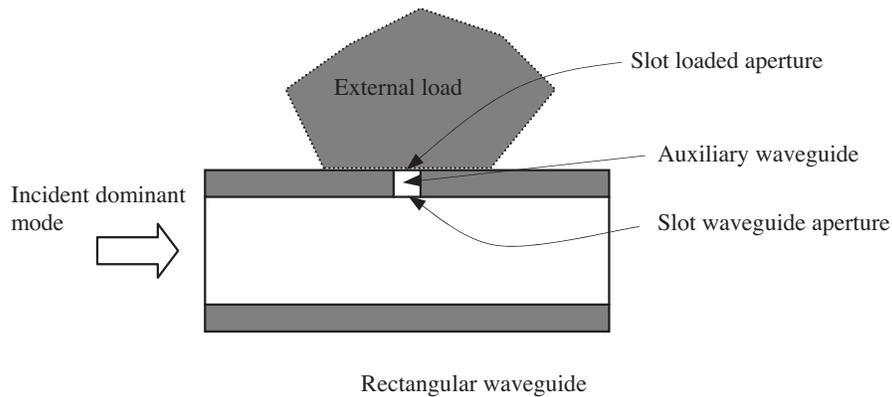
Rectangular waveguide

Figure 1. Waveguide slot in finite thickness wall loaded by arbitrary external load.

combination, of which the element values are functions of the aperture dimensions (the slot length and width) and the parameters of the host domain (the waveguide dimensions and material). The LC combination is coupled to the waveguide section by means of a transformer. In the special case of a slot coupler, the loaded aperture can be represented by an LC circuit. In general, however, the external load (the aperture and the external region) is modeled by some impedance, the value of which is determined by some algebraic manipulations on the pertinent MoM matrix. The proposed equivalent circuit outdoes the previous model in the fact that the parameters of the slot aperture equivalent circuit are not functions of the wall thickness or the load on the other side of the slot, and that the model can be used to solve problems with various loads on the other side of the slot with the same parameters obtained for the aperture in the waveguide.

In Section 2, brief description of the MoM solution will be given along with the algorithm of extracting the equivalent circuit parameters for a slot in zero-thickness walls. An extended model is subsequently developed in Section 3, where an auxiliary waveguide section is added to account for the wall thickness, and a transformer is introduced to achieve the proper impedance scaling between the main waveguide and the auxiliary waveguide section. The treatment of problems involving arbitrary loads excited by a waveguide slot is described in Section 4. In Section 5, results illustrating the application of the developed equivalent circuit models to a variety of problems are provided. Further conclusions are discussed in Section 6.

2. EQUIVALENT CIRCUIT MODEL FOR THE SLOT APERTURE: ZERO-THICKNESS WALL

In order to extract the circuit model parameters for the slot aperture in the host waveguide, the symmetric problem of a slot coupling two identical waveguides is considered. It is important to notice that the circuit parameters that will be obtained are not limited to analyzing the special case of two identical waveguides. It will be shown in the sections to follow that this model is indeed independent of the external load, and will thus be used in the analysis of other structures.

Following the same procedure outlined in [11], the scattering parameters for the transverse broad wall slot coupler depicted in Fig. 2(a) are computed, upon obtaining the MoM solution, as a ratio of the scattered to the incident field. Thus, the scattering parameter
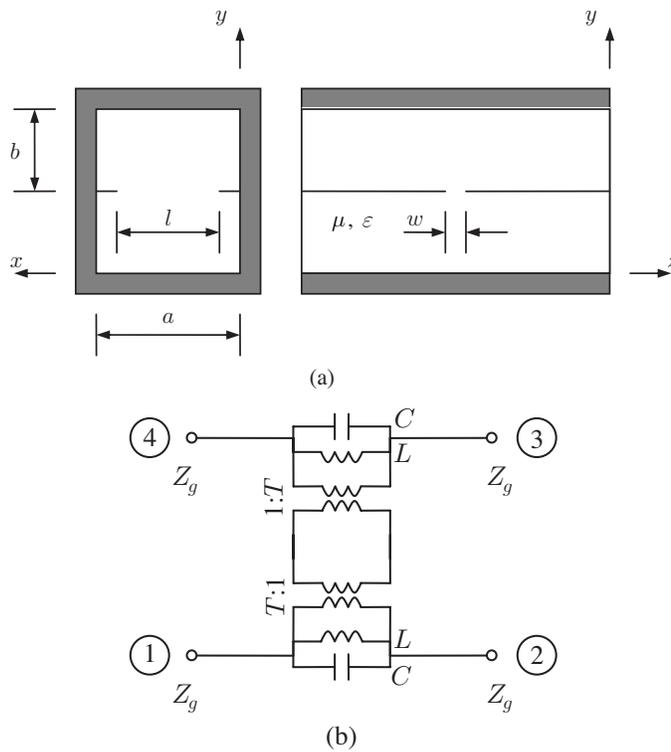

(a)

(b)

Figure 2. Transverse slot in the common broad wall of two identical waveguides: (a) original problem, and (b) equivalent circuit.

S_{11} may be obtained as

$$S_{11} = - \left. \frac{\hat{\mathbf{x}} \cdot \mathbf{H}_{10}^s}{\hat{\mathbf{x}} \cdot \mathbf{H}_{10}^i} \right|_{z=z_1}, \tag{1}$$

where $\mathbf{H}_{10}^s$ and $\mathbf{H}_{10}^i$ are the scattered and incident magnetic fields of the waveguide dominant mode, and $z = z_1$ is the reference plane of port 1.

The symmetry of the structure naturally suggests a symmetric equivalent circuit model as shown in Fig. 2(b), where every aperture (side) of the slot is modeled as an LC parallel combination, in contrast to the model proposed in [11]. The analysis of the circuit in Fig. 2(b) yields a reflection coefficient given by

$$S_{11} = \frac{1}{2(1 + 2Y_p Z_g)}, \quad Y_p = j\omega C + \frac{1}{j\omega L}, \tag{2}$$

where Z_g is the waveguide characteristic impedance based on the power-voltage definition defined by

$$Z_g = \frac{Z_0}{\sqrt{1 - (f_c/f)^2}}, \quad Z_0 = 2\sqrt{\frac{\mu}{\varepsilon}} \left(\frac{b}{a} \right), \tag{3}$$

where $f_c = 1/(2a\sqrt{\mu\varepsilon})$ is the cutoff frequency of the waveguide dominant mode.

Using the value of S_{11} from (1) at two frequency points, the equivalent inductance and capacitance of the slot aperture may be found as

$$C = \frac{\omega_1 \sigma_1 - \omega_2 \sigma_2}{\omega_1^2 - \omega_2^2}, \quad L = \frac{1/\omega_2^2 - 1/\omega_1^2}{\sigma_1/\omega_1 - \sigma_2/\omega_2}, \tag{4}$$

where

$$\sigma(\omega) = -\frac{1}{2Z_g} \frac{\mathrm{Re}(S_{11})}{\mathrm{Im}(S_{11})}, \quad \sigma_i = \sigma(\omega_i). \tag{5}$$

Alternatively, the values of L and C may be obtained as an optimum solution for a number of frequency points. The turns ratio T for the transformers shown in Fig. 2 can assume any value for the case of zero-thickness wall, since their effects annihilate one another and there is no change in the impedance definition in either waveguide.

A similar procedure may be followed to determine the circuit parameters for the centered horizontal end wall slot coupler shown in Fig. 3(a). From the equivalent circuit model of Fig. 3(b), the scattering parameter S_{11} is given by

$$S_{11} = -\frac{Y_p Z_g}{1 + Y_p Z_g}, \quad Y_p = j\omega C + \frac{1}{j\omega L}, \tag{6}$$
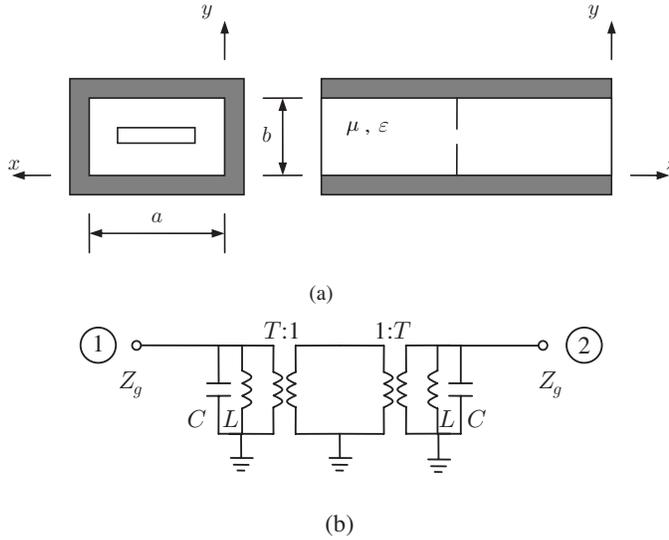
(a)

(b)

Figure 3. Horizontal end wall slot coupling two waveguides: (a) original problem, and (b) equivalent circuit.

and the expressions for the inductance and capacitance in this case will be the same as in (4), but with $\sigma(\omega)$ defined as

$$\sigma(\omega) = \frac{1}{Z_g} \frac{\text{Re}(S_{11})}{\text{Im}(S_{11})}. \tag{7}$$

The values obtained for the inductance and capacitance of the waveguide slot aperture can thus be used in the analysis of other problems, where the external load is not necessarily another identical waveguide. For example, the problem of a T-junction coupler shown in Fig. 4 can be solved using the models for the transverse and horizontal slot obtained using the above-mentioned approach. This suggests that viewing the slot as two separate apertures, each in its own environment, is justifiable. The values of the transformer turns ratios used in the equivalent circuits are obtained through the analysis of the problems with finite wall thickness as described in the next section.

3. EFFECT OF WALL THICKNESS

In the case of finite-thickness walls, a waveguide section of length t equal to the wall thickness is added to the equivalent circuit model using the waveguide components in ADS [1] as shown in Fig. 5 for
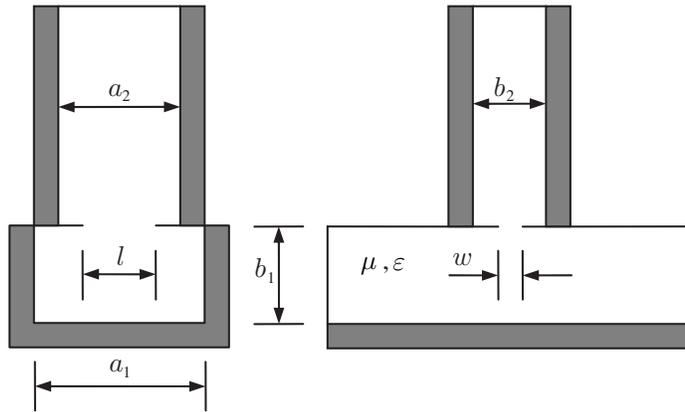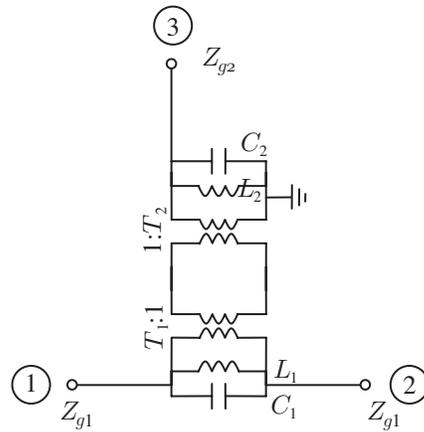
Figure 4. T-junction slot coupler: (a) original problem, and (b) equivalent circuit.

the case of the transverse slot coupler. Here, the transformer ratio T should be assigned a value that accounts for the change in impedance definition from one domain to the other. From the analysis of the T-junction problem of Fig. 4, with the secondary waveguide having the same cross-sectional dimensions as the slot, i.e., $a_2 = l$ and $b_2 = w$, an approximate expression for the transformer turns ratio may be found as

$$T^2 \approx 2\frac{l/a}{w/b}\sqrt{\left|\frac{1 - (\pi/l)^2(LC/\mu_s\varepsilon_s)}{1 - (\pi/a)^2(LC/\mu\varepsilon)}\right|}|S_{11}|_{f=f_{res}}, \tag{8}$$
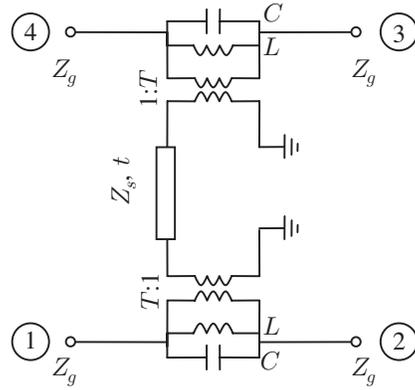
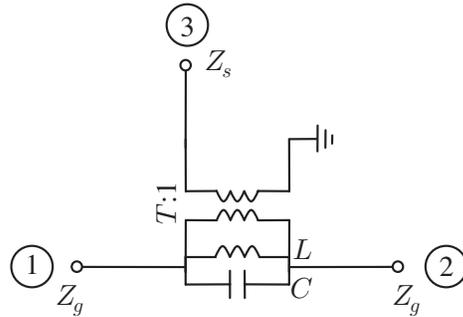**Figure 5.** Equivalent circuit model for a transverse slot coupler in thick wall.

Figure 6. Equivalent circuit for the T-junction problem used to estimate the transformer turns ratio.

where $f_{res} = 1/(2\pi\sqrt{LC})$ is the slot resonance frequency.

An interesting phenomenon that can be easily explained in terms of the equivalent circuit model (shown in Fig. 6) for the case where the secondary waveguide has the same dimensions as the slot is the total reflection that occurs while varying the source frequency at a frequency higher than the slot resonance frequency and lower than the cutoff frequency of the secondary waveguide. In view of the equivalent circuit, the inductive impedance of the waveguide below cutoff reduces the overall inductance of the resonant circuit, and thus increases the overall resonance frequency. After cutoff, the secondary waveguide impedance exhibits resistive behavior, with relatively small value compared to the main waveguide impedance, and thus most of the power is transmitted

through the main waveguide. This can be readily seen by considering the reflection coefficient at port 1 of the circuit of Fig. 6, given by

$$S_{11} = \frac{1}{1 + 2\frac{Z_g}{T^2 Z_s}(T^2 Y_p Z_s + 1)}. \tag{9}$$

From (9), S_{11} will equal unity, at the frequency that makes $T^2 Y_p Z_s$ equal to -1. At this frequency, the circuit made up of the slot inductance and capacitance and the waveguide inductive impedance will resonate, resulting in an open-circuit between ports 1 and 2 in Fig. 6.

4. EXCITATION OF ARBITRARY LOAD

Waveguide slots are often used to excite loads for which an equivalent circuit might not be easily constructed in contrast to waveguide loads. Thus, a general approach is to assume that this load is modeled by the MoM matrix, for which the order is equal to the number of unknowns on the slot. Assuming that the excitation (the tangential magnetic field on the lower surface of the slot loaded aperture) is known, then the problem for the external load shown in Fig. 1 may be reduced to the matrix form using the standard MoM procedure as

$$\mathbf{Y}^{ext}\mathbf{V} = \mathbf{I}, \tag{10}$$

where $\mathbf{Y}^{ext}$ and $\mathbf{I}$ are the MoM matrix and excitation vector, respectively.

For the equivalent circuit model shown in Fig. 7, only one of these unknowns (voltages) need to be incorporated in the circuit to model the load as per the compensation theorem, or equivalently a load impedance that will maintain the same load voltage in the circuit.

Assuming that the center unknown (voltage) $V_{\frac{N+1}{2}}$ is an appropriate representation of the external load, the solution of (10) provides a good estimate for the load impedance as

$$Z_L = Z^{ext}_{\frac{N+1}{2}, \frac{N+1}{2}}, \tag{11}$$

where $\mathbf{Z}^{ext} = (\mathbf{Y}^{ext})^{-1}$, and N (odd) is the number of unknowns on the slot. However, to take into consideration the interaction between the slot voltages, and assuming that the excitation is almost uniform for transverse slots, a better estimate for the load impedance may be computed as the average of the center row of $\mathbf{Z}^{ext}$, i.e.,

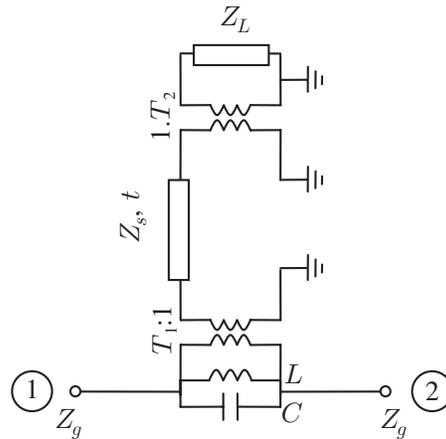$$Z_L = \frac{1}{N} \sum_{n=1}^{N} Z^{ext}_{\frac{N+1}{2}, n}. \tag{12}$$

Figure 7. Arbitrary load excited by the waveguide slot.

5. RESULTS

To illustrate the generality of the models obtained for the transverse and horizontal waveguide slots, Figs. 8 through 10 compare the results obtained using the circuit model and the MoM solution of the problems of a broad wall transverse coupler, an end wall horizontal coupler, and a T-junction coupler, respectively. Notice that the values of the L's and C's obtained for the transverse and horizontal slot from the first and second problem, respectively, are the same values used in the analysis of the third problem. The waveguides are standard X-band waveguides with cross-sectional dimensions $a_1 = a_2 = 22.86$ mm and $b_1 = b_2 = 10.16$ mm.

The total reflection phenomenon that is expected to happen for the T-junction in the case of a secondary waveguide having the same size as the slot can be seen in Fig. 11, where S_{11} peaks approximately at 9.37 GHz, a frequency higher than the slot resonance frequency and lower than the cutoff frequency of the secondary waveguide cutoff frequency, which are 8.80 GHz and 9.375 GHz, respectively.

An example where the load is not modeled using lumped circuit elements is that of waveguide slots radiating in free-space or exciting another radiator, such as a dielectric resonator antenna. Fig. 12 compares the scattering parameters of a transverse slot radiator obtained using the treatment outlined in Section 4 and the MoM solution of the whole problem. It is interesting to notice that the turns ratio T_2 that couples the auxiliary waveguide to the external load is
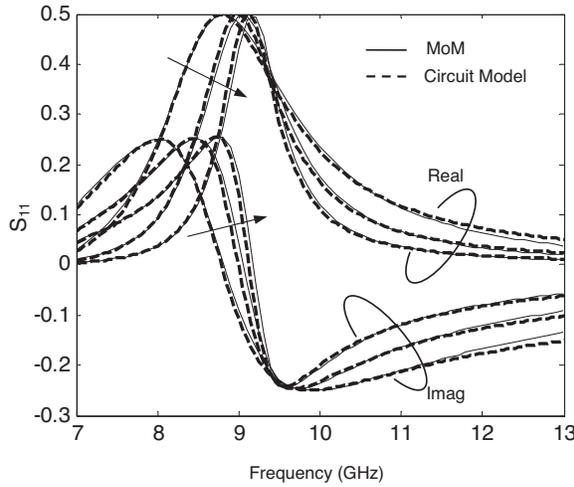
Figure 8. Return loss for a centered transverse broad wall slot coupler. Slot dimensions: $l = 16$ mm, $w = 1.5$ mm; circuit parameters: $L = 3.824$ nH, $C = 86.0$ fF, $T = 0.79$. The arrows indicate the direction of increasing wall thickness: $t = 0.0$ mm, 1.27 mm, and 3.0 mm.
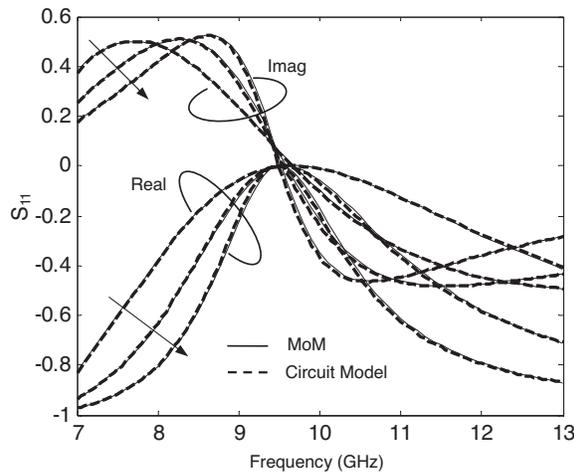

Figure 9. Return loss for a centered horizontal end wall slot coupler. Slot dimensions: $l = 16$ mm, $w = 1.5$ mm; circuit parameters: $L = 4.656$ nH, $C = 58.3$ fF, $T = 0.79$. The arrows indicate the direction of increasing wall thickness: $t = 0.0$ mm, 1.27 mm, and 3.0 mm.
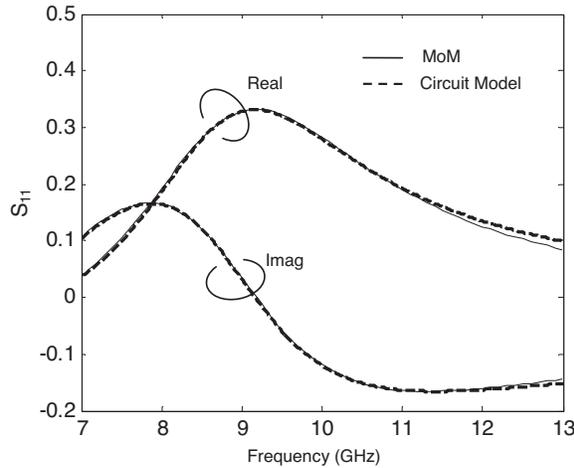
Figure 10. Return loss for a T-junction slot coupler. Slot dimensions: $l = 16\,\text{mm}$, $w = 1.5\,\text{mm}$, and $t = 0.0\,\text{mm}$.

virtually constant and approximately equal to 0.82 independent of the slot dimensions, the number of unknowns on the slot, or the nature of the external load. This was verified by considering a variety of loads including different waveguides, free-space, and dielectric resonators. A comparison with measured return loss for a transverse slot on the broad wall of a short-circuited waveguide is shown in Fig. 13. In Fig. 14, the scattering parameter S_{11} is depicted for the case of a stacked dielectric resonator antenna excited by a centered transverse slot with different materials filling the slot. The antenna is made up of two circular disks having the same axis of symmetry. The lower disk has a radius, height and relative permittivity of 6.5 mm, 5.5 mm, and 4.1, respectively, and the respective upper disk parameters are 3.5 mm, 2.8 mm, and 12.3. The slot is centered with respect to the waveguide broad wall and the dielectric disks.

The variation of the equivalent inductance and capacitance of a centered transverse broad wall slot aperture in an X-band waveguide with the slot length and width are depicted in Fig. 15. Similar curves for a centered horizontal end wall slot are shown in Fig. 16. Using curve-fitting techniques, expressions for the normalized inductance and capacitance as a function of the slot length and width were obtained as

$$\omega_c L_t / Z_0 = \sum_{m=0}^{M} \sum_{n=0}^{N} \Lambda_{mn}^t \exp(\frac{mw}{a}) \cos(\frac{n\pi l}{a}),$$

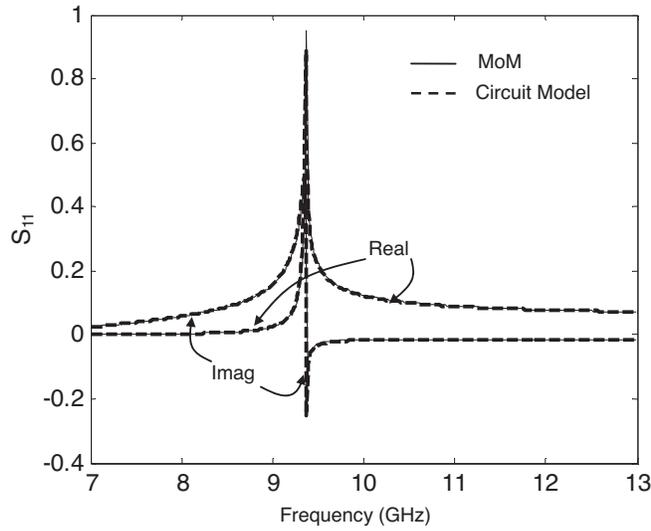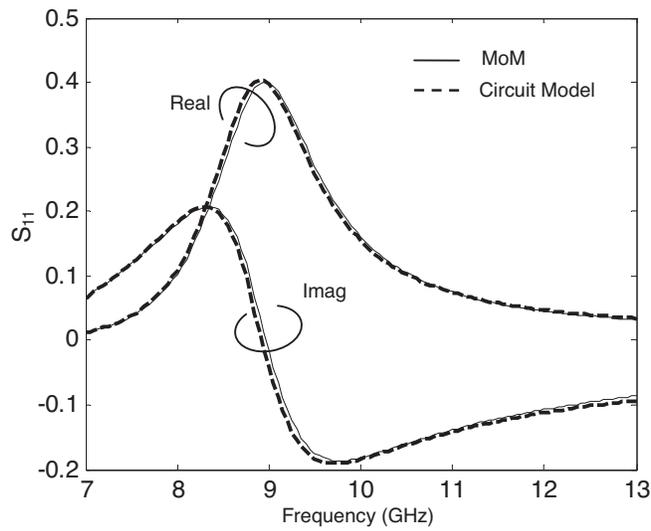**Figure 11.** Return loss for the T-junction with $a_2 = l$ and $b_2 = w$. Slot dimensions: $l = 16\,\text{mm}$, $w = 1.5\,\text{mm}$.

Figure 12. Scattering parameters of a centered transverse slot radiator. Slot dimensions: $l = 16\,\text{mm}$, $w = 1.5\,\text{mm}$, $t = 1.27\,\text{mm}$.
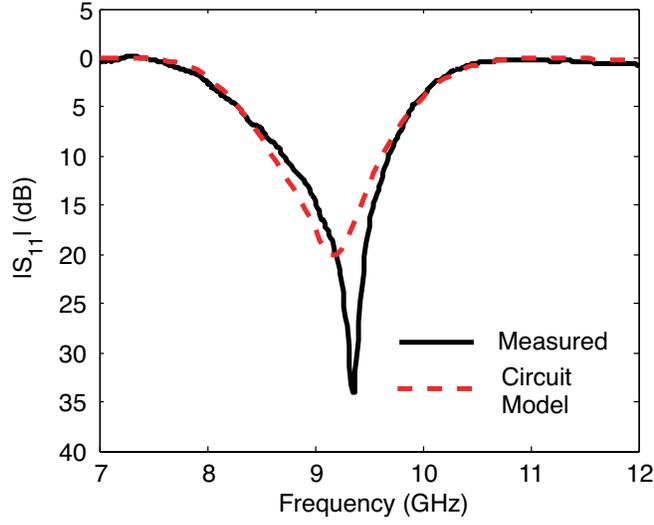
Figure 13. Return loss for a centered transverse slot antenna. Slot dimensions:$l = 15.8$ mm, $w = 1.58$ mm, $t = 1.27$ mm. The slot is at 25 mm from waveguide short-circuit termination.
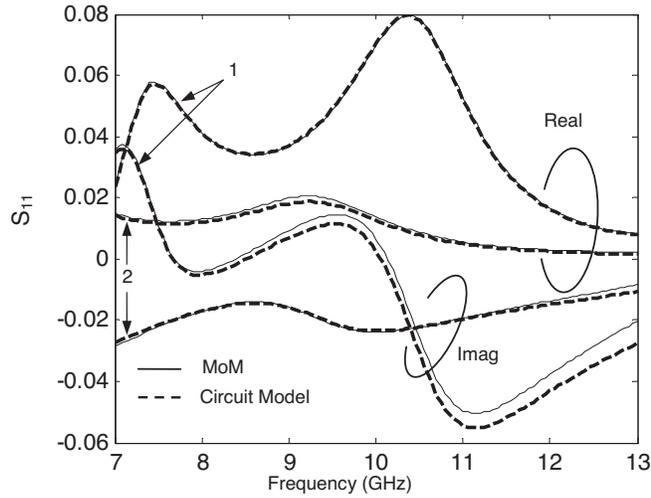

Figure 14. Scattering parameters of a centered transverse slot loaded with a stacked dielectric resonator antenna. Circuit parameters: $L = 1.528$ nH, $C = 127.3$ fF, $T = 0.62$ Slot parameters: $l = 12$ mm, $w = 1.0$ mm, $t = 1.27$ mm, and (1) $\varepsilon_s = 1.0$, (2) $\varepsilon_s = 4.1$.

Table 1. Coefficients for the expressions in (13).

	Λ^t_{mn}			Ψ^t_{mn}		
	$n = 0$	1	2	$n = 0$	1	2
$m = 0$	-10.49	4.92	-5.10	110	61	16
$m = 1$	18.18	-8.22	8.88	-241	-134	-35
$m = 2$	-7.48	3.17	-3.68	135	75	19
	Λ^h_{mn}			Ψ^h_{mn}		
	$n = 0$	1	2	$n = 0$	1	2
$m = 0$	-4.83	9.09	0.46	123	55	12
$m = 1$	4.95	-16.67	-3.51	-271	-121	-26
$m = 2$	0.10	7.47	3.17	151	67	14

$$\omega_c C_t Z_0 = \sum_{m=0}^{M} \sum_{n=0}^{N} \Psi^t_{mn} \exp(\frac{-mw}{a}) \cos(\frac{n\pi l}{a}),$$

$$\omega_c L_h / Z_0 = \sum_{m=0}^{M} \sum_{n=0}^{N} \Lambda^h_{mn} \exp(\frac{mw}{a}) \cos(\frac{n\pi l}{a}),$$

$$\omega_c C_h Z_0 = \sum_{m=0}^{M} \sum_{n=0}^{N} \Psi^h_{mn} \exp(\frac{-mw}{a}) \cos(\frac{n\pi l}{a}) \tag{13}$$

where the coefficients Λ and Ψ are given in Table 1.

For the transformer turns ratio, it was found that it is the same for centered transverse and horizontal slots, and is only function of the slot length, i.e., independent of the slot width (for narrow slots). An approximate expression for the normalized turns ratio is given by

$$T\sqrt{\eta/Z_0} \approx 1.01(l/a) + 0.127. \tag{14}$$

These expressions can significantly facilitate the analysis and design of a variety of problems involving the use of slot arrays. Consider the problem of a waveguide power distribution network shown in Fig. 17, where the power in the main waveguide is distributed with desired ratios among the secondary waveguides through slots of unknown dimensions. Using the optimization feature in ADS [1] with the slots dimensions being the optimization parameters, and the equivalent circuit parameters tied to the slot dimensions using (13) and (14), the slot dimensions can be determined. As an example, with the optimization goal being uniform power distribution between 3 X-band secondary waveguides at 10 GHz, the slot lengths were found to be as
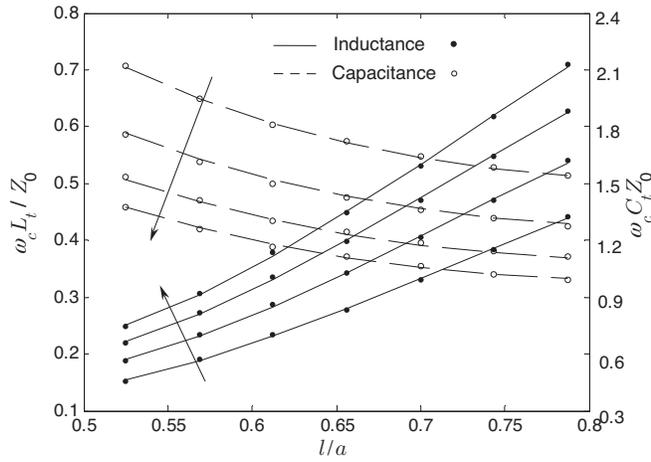
Figure 15. Variation of the normalized circuit parameters of the centered transverse broad wall slot with the normalized slot dimensions in an X-band rectangular waveguide. The arrows indicate the direction of increasing slot width: $w/a = 1/2a, 1/a, 3/2a, 2/a$. The dots and lines correspond to the actual values and curve-fitting values, respectively.

Figure 16. Variation of the normalized circuit parameters of the centered horizontal end wall slot with the normalized slot dimensions in an X-band rectangular waveguide. The arrows indicate the direction of increasing slot width: $w/a = 1/2a, 1/a, 3/2a, 2/a$. The dots and lines correspond to the actual values and curve-fitting values, respectively.
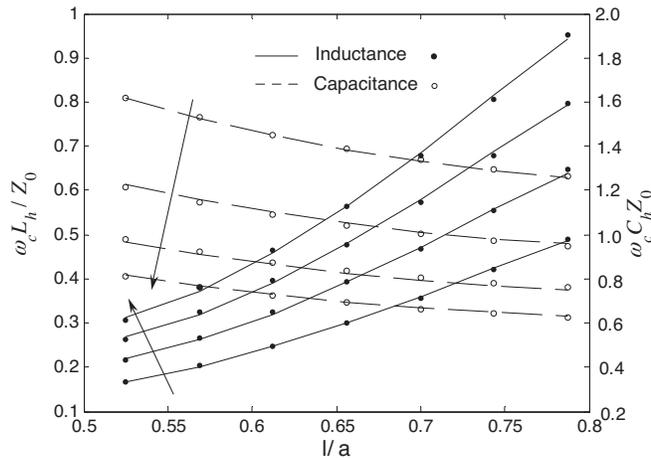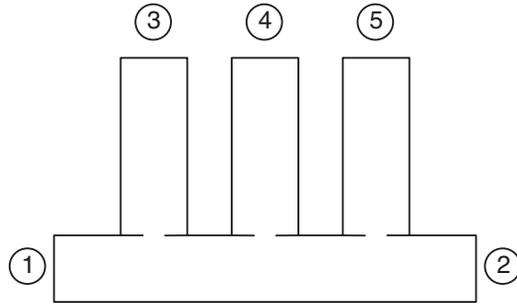
Figure 17. Waveguide distribution network: the main waveguide is coupled to the secondary waveguides through slots. Shown in the figure are the narrow walls of the waveguides.
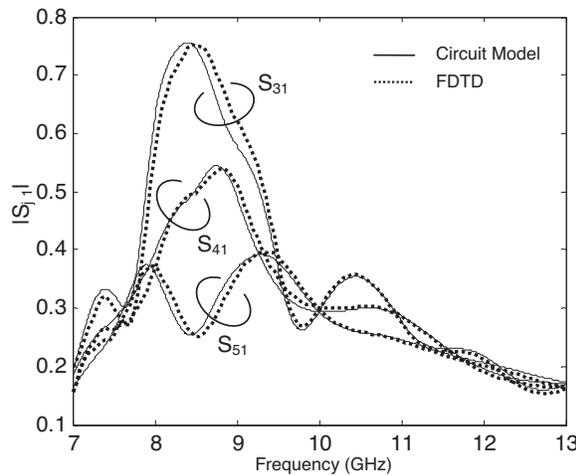

Figure 18. Scattering parameters for the distribution network of Fig. 17 using the dimensions listed in Table 2.

given in Table 2, assuming constant slot widths. The spacing between the slots is 40 mm, which is approximately equal to one waveguide wavelength at 10 GHz, and the wall thickness is 1.27 mm. Once the circuit parameters are known, the performance of the device at the whole frequency band of interest may be obtained from the circuit analysis. Comparison between the scattering parameters obtained from the circuit analysis and an FDTD-based commercial software [12] is shown in Fig. 18.

Table 2. Circuit parameters and physical dimensions of the slots used for uniform power distribution among 3 X-band waveguides.

	Slot #1	Slot #2	Slot #3
Length (mm)	17.72	17.56	17.49
Width (mm)	1.0	1.0	1.0
L_t (nH)	4.22	4.13	4.09
C_t (fF)	93.1	93.6	93.8
L_h (nH)	5.01	4.89	4.82
C_h (fF)	69.0	69.3	69.4
T	0.858	0.852	0.849

6. CONCLUSION

An LCT equivalent circuit model for waveguide slots was proposed and results obtained from the circuit analysis exhibited very good agreement with the full-wave solution over the entire band of interest. The use of this model to solve a variety of waveguide coupling and radiation problems was illustrated by the analysis and design of a number of waveguide slot-based structures.

Many tests were considered to verify the validity of the circuit model, and it was shown that varying the wall thickness or the parameters of the material filling the slot can be accounted for by adjusting the parameters of the auxiliary waveguide section, while keeping the slot equivalent inductance and capacitance unchanged. Modeling of arbitrary loads through some algebraic manipulations on the pertinent MoM matrix was also studied. Problems involving slot arrays were also considered, where the formulas for the slot parameters were employed to facilitate the synthesis problem. It is worth mentioning that the problems involving coupled external loads, which is the case for slot antenna arrays and arrays of slot-excited dielectric resonators, were not considered in this work, as they require taking the effect of the external mutual coupling; a problem that is beyond the scope of this paper. However, the use of the multiport Z-parameter matrix model is expected to properly characterize the coupled external loads.

The proposed modeling scheme can be extended to other slot configurations, such as longitudinal and compound slots, provided that the proper equivalent circuits are employed.

ACKNOWLEDGMENT

REFERENCES

1. Advanced Design System 2003A, User's Guide, Agilent Techn., 2003.
2. Elliott, R. S., *Antenna Theory and Design*, Prentice-Hall, Englewood Cliffs, NJ, 1981.
3. Elliott, R. S. and W. R. O'Loughlin, "The design of slot arrays including internal mutual coupling," *IEEE Trans. Antennas Propag.*, Vol. 34, No. 9, 1149–1154, 1986.
4. Casula, G. A. and G. Mazzarella, "A direct computation of the frequency response of planar waveguide slot arrays," *IEEE Trans. Antennas Propag.*, Vol. 52, No. 7, 1909–1912, 2004.
5. Mazzarella, G. and G. Montisci, "Wideband equivalent circuit of a centered-inclined waveguide slot coupler," *J. Electromagn. Waves Applicat.*, Vol. 14, 133–151, 2000.
6. Yee, H. Y., "The design of large waveguide arrays of shunt slots," *IEEE Trans. Antennas Propag.*, Vol. 40, No. 7, 775–781, 1992.
7. Stegen, R. J., "Slot radiators and arrays at X-band," *IEEE Trans. Antennas Propag.*, Vol. 1, No. 2, 62–64, 1952.
8. Elliott, R. S., "An improved design procedure for small arrays of shunt slots," *IEEE Trans. Antennas Propag.*, Vol. 31, No. 1, 48–53, 1983.
9. Eshrah, I. A., A. A. Kishk, A. B. Yakovlev, and A. W. Glisson, "Theory and implementation of dielectric resonator antenna excited by waveguide slot," *IEEE Trans. Antennas Propag.*, Vol. 53, No. 1, 483–494, 2005.
10. Eshrah, I. A., A. A. Kishk, A. B. Yakovlev, and A. W. Glisson, "Load-independent equivalent circuit model for transverse waveguide slots," *Proc. IEEE AP-S Int. Symp.*, Washington, D.C., USA, July 2005.
11. Eshrah, I. A., A. A. Kishk, A. B. Yakovlev, A. W. Glisson, and C. E. Smith, "Analysis of waveguide slot-based structures using wideband equivalent circuit model," *IEEE Trans. Microwave Theory Tech.*, Vol. 52, No. 12, 2691–2696, 2004.

12. QuickWave3D: A general purpose electromagnetic simulator based on conformal finite-difference time-domain method, v.2.2, QWED Sp. Z o.o, Dec. 1998.